Rev. Roum. Sci. Techn.– Électrotechn. et Énerg.
Vol. **67**, *2*, pp. 105–110, Bucarest, 2022

MULTILEVEL INVERTER FOR GRID-CONNECTED PHOTOVOLTAIC SYSTEMS

DALILA BERIBER[1], ABDELAZIZ TALHA[2], ABDELLAH KOUZOU[3], AMAR GUICHI[4], FARID BOUCHAFAA[5]

Keywords: Maximum power point; Boost converter; Photovoltaic; Grid, Multilevel; Fuzzy logic.

Abstract: In the last years, the increasing interest in substituting the conventional huge, centralized power generation systems with the distributed renewable energy sources has gained more attention; especially the photovoltaic (PV) distributed energy sources due to their various advantages and benefits. Besides, it becomes quite possible to produce a nearly sinusoidal output voltage waveform that satisfies the grid connection criteria by the use of multilevel voltage source inverters at the grid level. These types of inverters have known an important development that offers more advantages in comparison to their counterparts topologies where the produced ac output voltage is made up of several levels of voltages with lower THD content. In this context, a new power conversion structure is applied to the grid-connected photovoltaic systems where the three-phase three-level neutral point clamped (NPC) multilevel inverter is used. The modeling and the control of the grid-connected PV power system are investigated and each component of the system is presented and discussed in detail. The effectiveness of the proposed structure is checked with the obtained simulation results for the whole system using MATLAB/SIMULINK.

1. INTRODUCTION

Photovoltaic energy is considered the predominant and the main important renewable energy source because of its abundance, cleanness, ease of installation, and less maintenance [1]. However, the less efficiency of the photovoltaic (PV) panels and the high cost of the energy storage system restrains them from competing with the conventional energy sources. Accordingly, the performance of the PV systems still needs to be optimized. Among other ways, this can be done through the insertion of new topology converters to guarantee a real improvement in the efficiency of the PV system [2].

In the literature, several new power converter topologies have been developed to facilitate and encourage the integration of this type of energy source at all the network power system levels. Besides the generation of electrical energy, the electronics power based on high power conversion systems is mostly required to ensure the energy conversion and transmission under the suitable quality of energy [3], which in turn requires a high voltage rating semiconductor because of the high power which is needed. In the photovoltaic generation systems, the photovoltaic arrays (PVAs) are often connected in series with the conventional two-level inverter, where their mismatching reduces the generated power below its maximum point [4]. In order to overcome this deficit, these PVAs must be connected to a multilevel inverter. As part of the solution, the connection of PVAs to the three-level neutral point clamped [5] is suggested in this work where the pulse-width modulation control technology is used to independently control each of the voltages of the PVAs. Compared to the traditional two-level inverter system, the proposed method is intended to maximize the generated power of the system which will reduce the rated voltage of semiconductors, bound the output voltage distortion, and greatly improve the efficiency of the whole system.

The cell temperature and solar radiation have an important role in defining the main output nonlinear characteristics of the photovoltaic arrays. These two factors have a significant impact on the maximum power delivered by the photovoltaic generator [6] while, under a given condition, the PVAs have a unique maximum power point (MPP) that can be reached. For tracking this point, a dc-dc converter with maximum power point tracking, based on a fuzzy logic controller, is used. The rest of the paper is structured into seven sections and a conclusion. The second section is dedicated to the presentation of the PV system modeling, the third section presents the modeling of the dc-dc converter, the fourth section focuses on the application of fuzzy logic for ensuring the MPPT control, the PV grid connection system based on the multilevel inverter is presented in the fifth section, The presentation of the grid is explained in details in the sixth section, and section seven presents the simulation results and the discussions of the obtained results.

2. PHOTOVOLTAIC MODEL

The two-diode model of a solar cell is mainly composed of a light current source, two diodes, a series resistor, and a parallel resistor, as depicted in Fig. 1.

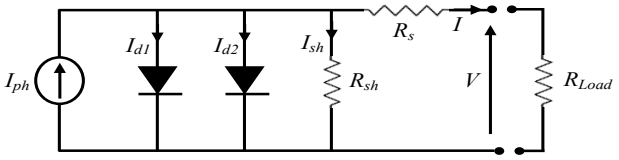

Fig. 1 – Equivalent electrical circuit of a cell.

The equation of the current-voltage characteristic of a solar cell is expressed as follows [7,8]:

$$I = I_{ph} - I_{s1}\left[\exp\left(\frac{q\left(V+R_S I\right)}{n_1 \mathrm{k} T}\right)-1\right] - I_{s2}\left[\exp\left(\frac{q\left(V+R_S I\right)}{n_2 V T}\right)-1\right] - \frac{V+R_S I}{R_{sh}}, \quad (1)$$

where I [A] is the solar-cell output current, I_{ph} [A] is the light-generated current, V [V] is the solar cell output

[1]Laboratory of Instrumentation, Faculty of Electronics and Computer Science, University of Sciences and Technology HouariBoumediene, BP 32 El-Alia, 16111 Bab-Ezzouar, Algiers, Algeria. dberiber@gmail.com
[2,5]Laboratory of Instrumentation, Faculty of Electronics and Computer Science, University of Sciences and Technology Houari Boumediene, BP 32 El-Alia, 16111 Bab-Ezzouar, Algiers, Algeria. abtalha@gmail.com, fbouchafa@gmail.com
[3]LAADI Laboratory, Faculty of Science and Technology, Djelfa University, Algeria. kouzouabdellah@ieee.org
[4]University of Mohamed Boudiaf, Faculty of Technology, BP. Box 166, M'sila, Algeria. guichi.omar@gmail.com

voltage, I_{s1} and I_{s2} [A] are respectively the first and the second diode reverse saturation current, n_1 and n_2 are the ideality factors of the two diodes, q = 1.6.10-19 C is the electronic charge, k = 1.3807.10-23 J·K^{-1} is Boltzmann's constant, T [K] is the cell temperature, R_{sh} [Ω] is the shunt resistance and R_s is the series resistance [Ω].

3. BOOST TYPE DC-DC CONVERTER

The intermediate stage between the photovoltaic generator (PVG) and the load presents a critical technological problem that limits the maximum generated power transfer between both sides. To overcome this problem, a power conversion interface system is used in this work; as a result, a controlled boost converter is chosen Fig. 2 [9,10].

When the main switch K of the used boost converter is turned on (conduction state or on the state), the current in the boost inductor L increases linearly, thus blocking the diode (blocked state or off state). When the switch K is turned off, the energy stored in the inductor is released through the diode D to the output $R_{Load}C_2$ circuit. The voltage produced at the output level of the boost converter is smoothed by the capacitive C_2 which corresponds to a low-pass filter and a nearly constant dc voltage is provided to the load [13,14].

4. FUZZY LOGIC MPP TRACKING CONTROLLER

The PV panel producing the maximum power strongly depends on the irradiation level and the cell temperature. Therefore, the maximum power point must be continuously tracked [13–15].

In addition to their multiple control applications, the fuzzy logic controllers (FLC) show interesting results in MPP tracking for PV systems. These kinds of controllers have some advantages compared to other used controllers in that their design is simple, their structure is robust, and they do not require a precise modeling system. However, complete information on the PV system operation is required by the designer to guarantee an optimal design. The fuzzy logic controller necessitates a definition of the main linguistic variables, such as PB (positive big), NB (negative big), ZA (zero approximately), NS (negative small), and PS (positive small) [7,15,16].

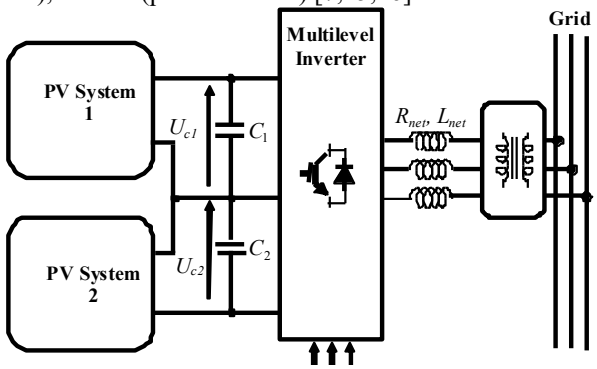

Fig. 3 – Grid connection of two PV systems with a three-level converter.

The two FLC input variables which are the discrete values of the error (E) and the change of error (CE) calculated at each sample time k are expressed as follows [13–15,17,18]:

$$\begin{cases} E(k) = \dfrac{P(k) - P(k-1)}{V(k) - V(k-1)} \\ CE(k) = E(k) - E(k-1) \end{cases}, \tag{2}$$

where $P(k)$ is the discrete instantaneous power of the photovoltaic generator.

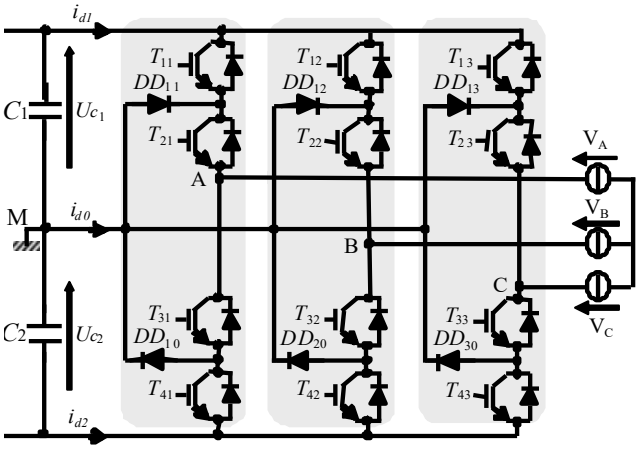

Fig. 4 – Schematic diagram of the multilevel NPC three-level inverter.

Different multilevel inverter topologies have been used in several high and medium power applications. However, the main three common basic topologies of multilevel inverters are the neutral-point clamped (NPC) multilevel inverters [20], the flying capacitor (FC) multilevel inverters [21], and the cascaded H-bridge (CHB) multilevel inverters [22]. In this work, a three-phase three-level NPC inverter is used. On the input side, the three phases are sharing the same dc-link supply which feeds two series of similar capacitors that include a common point "M" as shown in Fig .4. Each phase is presenting an arm; the arm is composed of four semiconductor switches that are divided into two sets (two half arms), the upper two and the lower two switches. The switch is composed of a transistor with an anti-parallel diode. For each phase, the midpoint of the lower set is connected to that of the upper one through two clamped diodes and the midpoint of these two diodes is connected to the common point of the series capacitors [5,7,23]. In this topology, the voltages across the two input capacitors must be kept symmetrical and equal to half the input dc voltage value representing the dc-dc boost converter output voltage. Indeed, each blocked transistor is subject to the voltage applied to the corresponding capacitor that equals half the input dc voltage. This can be considered an important feature of such inverter topology to be used in high-voltage high-power applications.

The output voltages of the inverter referred to as the middle point M is defined as follows [5,20]:

$$\begin{bmatrix} V_{AM} \\ V_{BM} \\ V_{CM} \end{bmatrix} = \begin{bmatrix} F_{11}^b \\ F_{21}^b \\ F_{31}^b \end{bmatrix} U_{C1} - \begin{bmatrix} F_{10}^b \\ F_{20}^b \\ F_{30}^b \end{bmatrix} U_{C2}. \tag{3}$$

The simple output voltages are also defined as follows [5]:

$$\begin{bmatrix} V_A \\ V_B \\ V_C \end{bmatrix} = \frac{1}{3}\begin{bmatrix} 2 & -1 & -1 \\ -1 & 2 & -1 \\ -1 & -1 & 2 \end{bmatrix}\left\{\begin{bmatrix} F_{11}^b \\ F_{21}^b \\ F_{31}^b \end{bmatrix} U_{C1} - \begin{bmatrix} F_{10}^b \\ F_{20}^b \\ F_{30}^b \end{bmatrix} U_{C2}\right\}. \quad (4)$$

The input currents of the inverter are given as follows [24]:

$$\begin{cases} i_{d1} = F_{11}^b i_1 + F_{21}^b i_2 + F_{31}^b i_3 \\ i_{d2} = F_{10}^b i_1 + F_{20}^b i_2 + F_{30}^b i_3 \end{cases}. \quad (5)$$

The current i_{d0} related to the common point of the series capacitors is defined by the following relation [5, 20]:

$$i_{d0} = (i_1 + i_2 + i_3) - (i_{d1} + i_{d2}), \quad (6)$$

where F_{i1}^b and F_{i0}^b are the phases of the half arms connection function associated respectively to the upper and lower half arm [5,20]:

$$\begin{cases} F_{11}^b = F_{11}F_{12} \\ F_{10}^b = F_{13}F_{14} \end{cases}; \quad \begin{cases} F_{21}^b = F_{21}F_{22} \\ F_{20}^b = F_{23}F_{24} \end{cases}; \quad \begin{cases} F_{31}^b = F_{31}F_{32} \\ F_{30}^b = F_{33}F_{34} \end{cases}, \quad (7)$$

where i presents the number of the leg, $i = \{1,2,3\}$.

The switch T_{ij} introduces a connection function F_{ij} that describes its state, such as $F_{ij} = 1$ when the switch T_{ij} is on (closed) and $F_{ij} = 0$ is the switch T_{ij} is off (opened), $j = \{1,2,3,4\}$.

The space vector modulation (SVM) strategy is used in the control of the multilevel chosen inverter by the adoption of the two bipolar carriers. This strategy is characterized by two parameters [24, 25]: the modulation index m ($m = f_p / f$) and the modulation rate r ($r = V_m/U_{pm}$).

6. ELECTRICAL GRID MODELING

The equivalent electrical circuit of the grid phase is shown in Fig. 5.

This circuit is composed of three elements in series, a voltage source V_{neti}, an inductance L_{net} and a resistor R_{net} [25]. Based on Park components and the equivalent circuit, the grid voltage can be expressed in the d-q frame as follows [26]:

$$\begin{bmatrix} V_{dnet} \\ V_{qnet} \end{bmatrix} = \begin{bmatrix} R_{net} & -L_{net}\omega \\ L_{net}\omega & R_{net} \end{bmatrix} \cdot \begin{bmatrix} i_d \\ i_q \end{bmatrix} + \begin{bmatrix} 0 & L_{net} \\ L_{net} & 0 \end{bmatrix} \cdot \frac{d}{dt}\begin{bmatrix} i_d \\ i_q \end{bmatrix} + \begin{bmatrix} V_d \\ V_q \end{bmatrix}, \quad (8)$$

where:

- V_d and V_q are the inverter output voltage components of d and q axis, respectively;
- V_{dnet} and V_{qnet} are the grid voltage components of d and q axis, respectively;
- i_d and i_q are the line current components of d and q axis, respectively;
- L_{net} and R_{net} are the grid inductance and resistance, respectively.

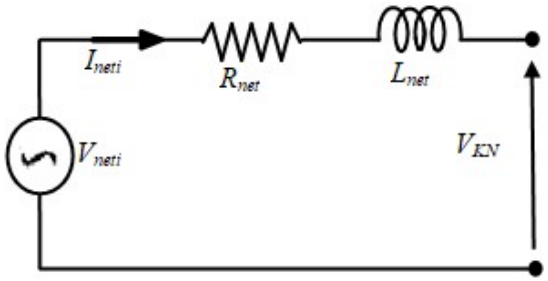

Fig. 5 – The equivalent electrical circuit of the grid phase.

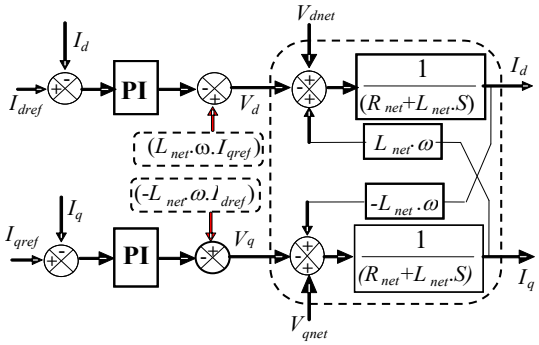

Fig. 6 – Grid current control by PI regulators.

Active and reactive powers can be expressed as a function of the Park components of the grid voltages and currents by the following expressions [5,27]:

$$\begin{cases} P_g = vnet_d\ inet_d + vnet_q\ inet_q \\ Q_g = vnet_d\ inet_q - vnet_q\ inet_d \end{cases}. \quad (9)$$

Based on equation (9), it is possible to control the active and the reactive power supplied to the grid by setting the reference currents according to the following equation [12,27]:

$$\begin{cases} is_{d\_ref} = \dfrac{P_{g_{ref}}\hat{v}net_d - Q_{g_{ref}}\hat{v}net_q}{\hat{v}_{sd}^{\,2} + \hat{v}_{sq}^{\,2}}, \\ is_{q\_ref} = \dfrac{P_{g_{ref}}\hat{v}net_q + Q_{g_{ref}}\hat{v}net_d}{\hat{v}net_d^{\,2} + \hat{v}net_q^{\,2}}. \end{cases} \quad (10)$$

Reference currents can be gathered in one vector:

$$Inet_{dq\_ref} = \left[inet_{d\_ref}, inet_{q\_ref}\right]^T. \quad (11)$$

The task of the dc-link voltage and the current control can be accomplished by using a Proportional-Integral (PI) controller, this choice has been carried out due to its good performance of the steady-state and dynamic behavior when used with the dc-ac converter [28]. Its transfer function can be expressed as follows:

$$H(S) = K \cdot \left(\frac{1 + T_i S}{T_i S}\right), \quad (12)$$

with

$$K = \frac{10\, R_{net}\, T_i}{T_e}, \quad (13)$$

where K is the controller gain, T_i is the integral action and T_e represents the time constant required for the current controller

$$T_e = \frac{L_{net}}{R_{net}}. \quad (14)$$

The coupling which exists between the two currents i_d and i_q makes the control of the established model very complex. To overcome this problem, a decoupling of the two parameters by compensation is applied, it consists in adding the terms $L_{net}\omega i_{qref}$ and $L_{net}\omega i_{dref}$ to the loop of the internal control. The control loops of the currents i_d and i_q are presented in Fig. 6.

7. SIMULATION RESULTS AND DISCUSSION

The boost converter presented in this study is controlled by a Fuzzy Logic controller to ensure the tracking of the maximum power point, whereas the three-level inverter is used to ensure the grid connection of the PV system. The boost converter is controlled based on a space vector modulation strategy using two bipolar carriers. The PV system is composed of two photovoltaic arrays of 16 series solar panels that can provide a power of 1500W.

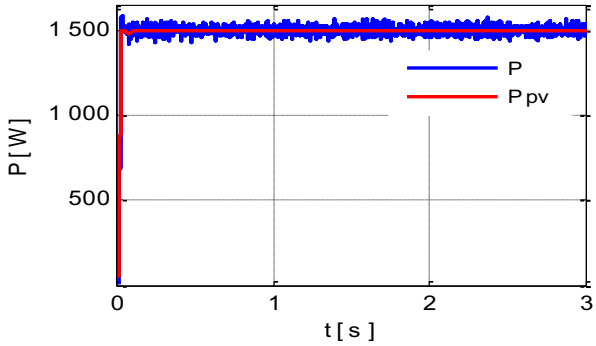

Fig. 7 – Grid active power and the produced power by the PV system.

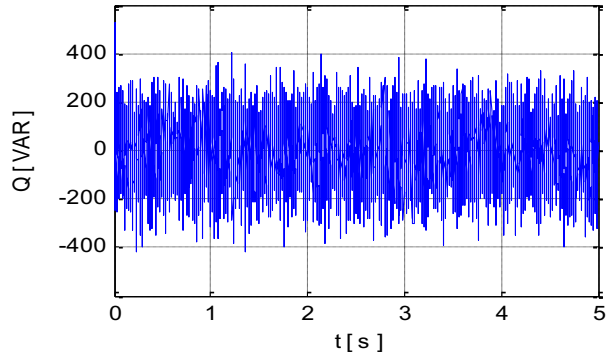

Fig. 8 – Grid reactive power.

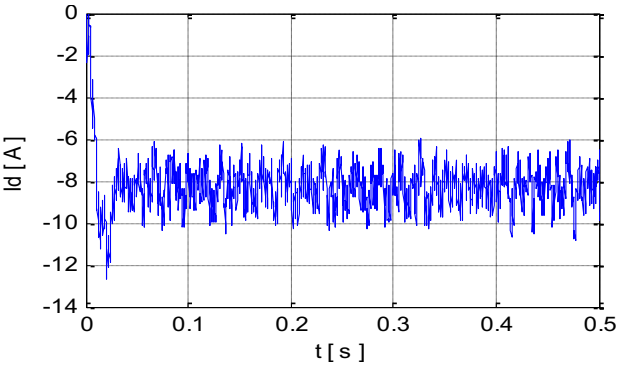

Fig. 9 – Direct current.

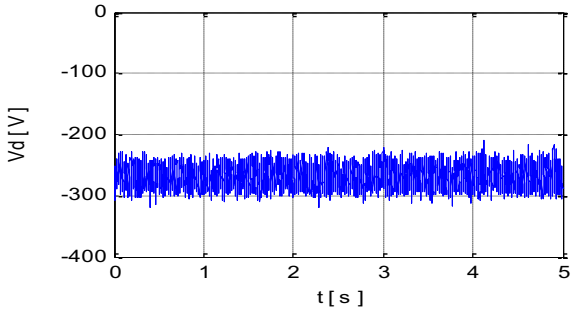

Fig. 10 – Direct voltage.

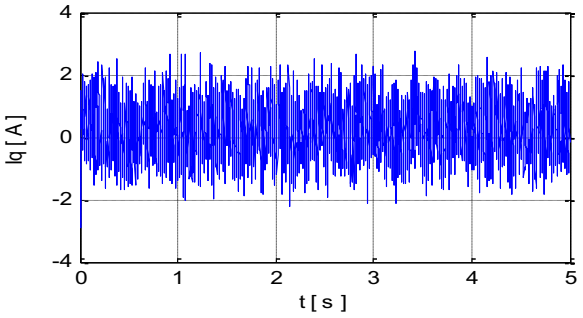

Fig. 11 – Quadratic current.

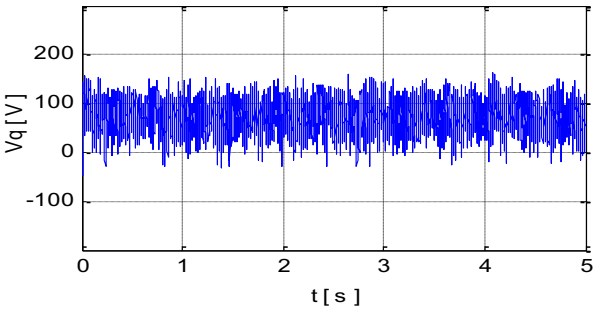

Fig. 12 – Quadratic voltage.

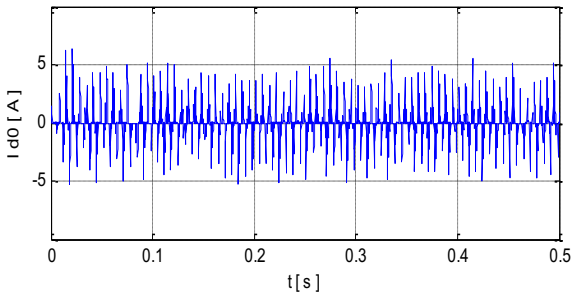

Fig. 13 – Input current i_{d0} of three – levels NPC inverter.

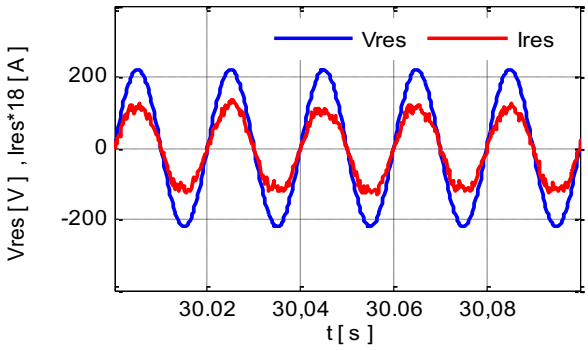

Fig. 14 – Output current of three - level NPC-VSI (18 times) and the grid voltage (V).

From the acquired results, it can be observed clearly that the active power follows its reference perfectly, as shown in Fig. 7, and the reactive power fits correctly the requirement of the grid connection control which has been set to be null as depicted in Fig. 8. The currents i_d and i_q reflect the behaviors of the active and reactive power, P and Q respectively, as illustrated in Fig. 9 and 11 whereas the corresponding voltages are presented in Fig. 10 and 12.

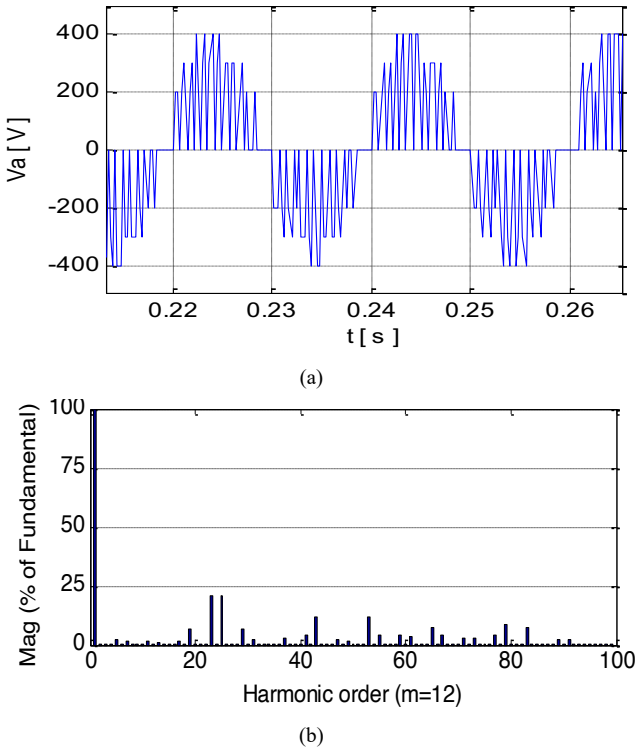

Fig. 15 – Characteristics of three - level NPC-VSI. (a) The output voltage. (b) The harmonic spectrum of the output voltage.

Practically, while the current i_{d0} has a zero average value as depicted in Fig.13, which means that the two input voltages are maintained in balance and the midpoint M is effectively kept at a zero voltage. From Fig. 14, the shift phase between the grid current and the grid voltage is negligible, which means that the unity power factor is perfectly achieved. On the other side, the grid injected current is nearly sinusoidal, and the harmonics spectrum of the inverter output voltage is reduced (THD = 20.39 %), especially if the evaluation is considered for low harmonics order (components with less than 1 kHz) as illustrated in Fig. 15. In addition, it can be clearly noted that the other current harmonics can be damped easily by the insertion of an appropriate output filter which is in the present case an inductor providing the connection between the three-level NPC-VSI and the grid at the point of common coupling Fig. 3. It can be said that the harmonics content in the current is practically neglected and the current THD is less than 4% which is aligned with the requirements of the standard.

8. **CONCLUSIONS**

This paper proposed a three-phase grid-connected photovoltaic system based on a three-phase three-level NPC multilevel to ensure the dc-ac conversion stage. Such topology is mainly used to achieve the requirements of the connection and the high-power transmission between the PV system power source and the main grid. This topology has remarkably proved its efficiency and suitability, and it offers several advantages compared to the conventional inverter topologies used in such applications, such as reduction of the output voltage harmonics, and unity power factor at the point of common coupling, and high efficiency. In addition, the integration of the fuzzy logic controller has clearly improved the overall system efficiency where the energy losses have been reduced during the frequent irradiation changes according to the main principle of the dc-dc converter control based on the MPPT algorithm.

The obtained results show the effectiveness and the efficiency of the proposed structure, as well as its control system which has been tested. At the same time, it can be said that the eventual cascaded multilevel converter can be an attractive and suitable choice for grid-connected PV systems and carries a substantial solution for the high-power application of the PV grid-connected systems.

ACKNOWLEDGMENTS

This work has been supported by la Direction Générale de la Recherche Scientifique et du Développement Technologique (DGRSDT), Ministère de l'Enseignement Supérieur et de la Recherche Scientifique de la République Algérienne Démocratique et Populaire.

Received on 25 May 2021.

REFERENCES

1. G. Tsantopoulos, G. Arabatzis, S. Tampakis, *Public attitudes towards photovoltaic developments: Case study from Greece*, Energy Policy., **71**, pp. 94–106 (2014).
2. J.A. Hernandez, D. Velasco, C.L. Trujillo, *Analysis of the effect of the implementation of photovoltaic systems like option of distributed generation in Colombia*, Renew. Sust Energy Rev., **15**, pp. 2290–2298 (2011).
3. Chen H, et al.: *Progress in electrical energy storage system: A critical review*, Progress in Natural Science, **10**, pp. 291–312 (2009).
4. J. Alonso-Martinez, J. Eloy-Garcia, S. Arnaltes, *Direct power control of grid-connected PV systems with three-level NPC inverter*, Sol. Energy, **84**, pp. 1175–1186 (2010).
5. H. Boumaaraf, A. Talha, O. Bouhali, *A three-phase NPC grid-connected inverter for photovoltaic applications using neural network MPPT*, Renew. Sust Energy Rev., **49**, pp. 1171-1179 (2015).
6. S.B. Kjaer, J. Pedersen, F. Blaabjerg, *A review of single-phase grid-connected inverters for photovoltaic modules*, IEEE Trans. Ind. Appl., **41**, pp. 518–523 (2005).
7. C. Garrido-Alzar, *Algorithm for extraction of solar cell parameters from I-V curve using double exponential model*, Renew. Energ., **10**, pp. 125-128 (1997).
8. M. Hejri, H. Mokhtari, M. R. Azizian, M. Ghandhari, L. Soder, *On the parameter extraction of a five-parameter double-diode model of photovoltaic cells and modules,* IEEE J. Photovolt., **4**, 3, pp. 915–923 (2014).
9. K. Sundareswaran, P. Sankar, P. Nayak, *MPPT of PV systems under partially shaded conditions through a colony of flashing fireflies*, IEEE Trans. Energy Convers., **29**, pp. 463–472 (2014).
10. G. Saravana Ilango, P. Srinivasa Rao, A. Karthikeyan, C. Nagamani, *Single-stage sine-wave inverter for an autonomous operation of solar photovoltaic energy conversion system*, Renew. Energy, **35**, pp. 275–282 (2010).
11. H. Fathabadi, *Novel high-efficiency dc/dc boost converter for using in photovoltaic systems*, Sol. Energy, **125**, pp. 22–31 (2016).
12. A. Robert, H, Turton, T., Casten, *Energy efficiency, sustainability and economic growth*, Energy, **32**, pp. 634–648 (2007).
13. H. Boumaaraf, A. Talha, O. Bouhali, *Maximum power point tracking using neural networks control for grid-connected photovoltaic system*, 4th International Conference on Power Engineering,

Energy and Electrical Drives, POWERENG 2013, Istanbul, Turkey, 13-17 May 2013.
14. A. Panda, M.K. Pathak, *Fuzzy intelligent controller for the maximum power point tracking of a photovoltaic module at varying atmospheric conditions*; J. Energy Techno. Policy, **2**, pp. 18–27 (2011).
15. B.A. Alajmi, K.H. Ahmed, S.J. Finney, B.W. Williams, *Fuzzy-logic-control approach of a modified hill-climbing method for maximum power point in microgrid standalone photovoltaic system*, IEEE Trans. Power Electron., **26**, pp. 1022–1030 (2011).
16. K. Loukil, H.Abbes, H. Abida, M. Abid, A.Toumi, *Design and implementation of reconfigurable MPPT fuzzy controller for photovoltaic systems,* Ain Shams Engin. Journal, **11**, *2*, pp. 319–328 (2020).
17. A. El Khateb, N. Abd Rahim, J. Selvaraj, M. Nasir Uddin, *Fuzzy-Logic-Controller-Based SEPIC Converter for Maximum Power Point Tracking*, IEEE Trans. Ind. Appl., **50**, pp. 2349–2358 (2014).
18. A. Laib, F. Krim, B. Talbi, H. Feroura, A. Belaout, *Hardware implementation of fuzzy maximum power point tracking through sliding mode current control for photovoltaic systems*, Rev. Roum. Sci. Techn.– Électrotechn. et Énerg., **66**, *2*, pp. 91–96 (2021).
19. S. Thamizharasan, J. Baskaran, S. Ramkumar, S. Jeevananthan, *Cross-switched multilevel inverter using auxiliary reverse-connected voltage sources*, IET Power Electr, **7**, pp. 1519–1526 (2014).
20. S. Alepuz, S. Busquets-Monge, J. Bordonau, J. Gago, D. Gonzalez, J. Balcells, *Interfacing renewable energy sources to the utility grid using a three-level inverter*, IEEE Trans. on Ind. Electron., **53**, pp. 1504–1511 (2006).
21. J. Ebrahimi, E. Babaei, G.B. Gharehpetian, *A new multilevel converter topology with a reduced number of power electronic components*, IEEE Trans. Ind. Elect., **59**, pp. 655–667 (2010).
22. A. Talha, H. Boumaaraf, O. Bouhali, *Evaluation of maximum power point tracking methods for photovoltaic systems*, Archives of Control Sciences, **21**, pp. 151–165 (2011).
23. D.W. Kang, B.K. Lee, J.H. Jeon, T.J. Kim, D.S. Hyun, *A symmetric carrier technique of CRPWM for voltage balance method of flying capacitor multilevel inverter*, IEEE Trans. on Ind. Electron., **52**, pp. 879–888 (2005).
24. B. Xiao, , L. Hang, J. Mei, C. Riley, L.M. Tolbert, B. Ozpineci, *Modular cascaded H-bridge multilevel PV inverter with distributed MPPT for grid-connected application*, IEEE Trans. on Ind. Appl., **51**, 1722–1731 (2015).
25. A. Talha, *Etude de différentes cascades de l'onduleur a sept niveaux a structure NPC. Application a la conduite d'une machine synchrone a aimants permanents*, 2004, Thèse de Doctorat, Ecole Nationale Polytechnique, Alger, Algérie.
26. L. Tolbert, F.Z. Peng, T.G. Habetler, *Multilevel PWM methods at low modulation indices*, IEEE Trans. on Power Electron., **15**, pp. 719–725 (2000).
27. F. Blaabjerg, R. Teodorescu, M. Liserre, V. Timbus Adrian, *Overview of control and grid synchronization for distributed power generation systems*, IEEE Trans. Power Electron., **53**, pp. 1398–1409 (2006).
28. O. Aouchenni, R. Babouri, K. Ghedamsi, D. Aouzellag, *Wind farm based on doubly fed induction generator entirely interfaced with power grid through a multilevel inverter,* Rev. Roum. Sci. Techn.– Électrotechn. et Énerg. **62**, *2*, pp. 170–174 (2017).
29. M. Dali, J. Belhadj, X. Roboam, *Hybrid solar-wind system with battery storage operating in gride connected and standalone mode: control and energy management-experimental investigation*, Energy, **35**, pp. 2587–2595 (2010).